Monthly Notices
of the
ROYAL ASTRONOMICAL SOCIETY

MNRAS **492,** 1–7 (2020)
Advance Access publication 2019 October 23

doi:10.1093/mnras/stz2972

Discovery of a large H I ring around the quiescent galaxy AGC 203001

Omkar Bait [1]★ Sushma Kurapati,[1] Pierre-Alain Duc,[2] Jean-Charles Cuillandre,[3] Yogesh Wadadekar,[1] Peter Kamphuis[4] and Sudhanshu Barway [5]

[1]*National Centre for Radio Astrophysics, Tata Institute of Fundamental Research, Post Bag 3, Ganeshkhind, Pune 411007, India*
[2]*Universitè de Strasbourg, CNRS, Observatoire Astronomique de Strasbourg, UMR 7550, F-67000 Strasbourg, France*
[3]*AIM, CEA, CNRS, Universitè Paris-Saclay, Universitè Paris Diderot, Sorbonne Paris Citè, Observatoire de Paris, PSL University, F-91191 Gif-sur-Yvette Cedex, France*
[4]*Astronomisches Institut Ruhr-Universität Bochum (AIRUB), Universitätsstrasse 150, D-44780 Bochum, Germany*
[5]*Indian Institute of Astrophysics (IIA), II Block, Koramangala, Bengaluru 560 034, India*

Accepted 2019 October 18. Received 2019 October 6; in original form 2019 June 26

ABSTRACT

Here we report the discovery with the Giant Metrewave Radio Telescope of an extremely large (∼115 kpc in diameter) H I ring, located around a massive quenched galaxy, AGC 203001, but off-centred with respect to it. This ring does not have any bright extended optical counterpart unlike several other known ring galaxies. Our deep *g*-, *r*-, and *i*-band optical imaging of the H I ring, using the MegaCam instrument on the Canada–France–Hawaii Telescope, shows however several regions with faint optical emission at a surface brightness level of ∼28 mag arcsec^{-2}. Such an extended H I structure is very rare with only one other case known so far – the Leo ring. Conventionally, off-centred rings have been explained by a collision with an 'intruder' galaxy leading to expanding density waves of gas and stars in the form of a ring. However, in such a scenario the impact also leads to large amounts of star formation in the ring that is not observed in the ring presented in this paper. We discuss possible scenarios for the formation of such H I-dominated rings.

Key words: galaxies: evolution – galaxies: general – galaxies: groups: general – galaxies: interactions.

1 INTRODUCTION

Ring galaxies have been studied in the optical for a long time, starting with the now famous 'Cartwheel' ring (Zwicky 1941). This ring harbours a wide range of features like a bright blue ring, spokes, an inner secondary ring, and a nucleus. The first breakthrough in understanding their origin came from Lynds & Toomre (1976) and Theys & Spiegel (1977) who showed that such rings could form due to a density wave from a head-on high-speed collision with an intruder galaxy. Such rings, which are classified as P-type rings (also termed as collisional rings), typically have an off-centre nucleus and a knotty structure (Few & Madore 1986). They differ from another class of ring galaxies, termed as O-type rings, which have a central nucleus and a smooth profile (Few & Madore 1986) and are believed to have formed due to Lindblad resonances (de Vaucouleurs 1959; Binney & Tremaine 2008). The strong impact in collisional rings leads to a burst of star formation (SF) in the whole system (Appleton & Struck-Marcell 1987; Struck-Marcell & Appleton 1987). It was shown in a recent simulation of a Cartwheel-like galaxy that the location of active SF follows a particular sequence, wherein SF is first enhanced in the ring shortly after the interaction, then in the spokes, and finally in the nucleus (Renaud et al. 2018). Collisional rings are also known to form knots due to their self-gravity, a phenomenon known as 'bead instability' (Dyson 1893), as first pointed out by Theys & Spiegel (1977) and also seen in a more detailed simulation by Hernquist & Weil (1993). This leads to the fragmentation of the ring in about 100 Myr (Theys & Spiegel 1977) and it fades almost completely in about 0.5 Gyr (Mapelli et al. 2008), thus making the ring fairly short-lived. Interestingly, such collisional rings are also produced in large-scale cosmological simulations whose SF properties are found to be consistent with observations (Snyder et al. 2015; Elagali et al. 2018).

It is well known that early-type galaxies (ETGs) can host H I (e.g. van Driel & van Woerden 1991; Oosterloo et al. 2002, 2010; Morganti et al. 2006; Serra et al. 2012), even more so in non-cluster environments, in a variety of morphologies ranging from settled, unsettled discs/rings to disturbed morphologies (Serra et al. 2012). In cases where large amounts of H I is hosted by ETGs, it is known to be distributed in the form of large ring/disc morphology (e.g. Morganti et al. 2003b; Serra et al. 2012) with signs of recent SF in it (Yıldız et al. 2017). Among them, there is one case of an optically devoid large H I ring – the 'Leo ring' (Schneider et al. 1983, 1989; Schneider 1985). Here, the H I is distributed in the

★ E-mail: omkar@ncra.tifr.res.in

© 2019 The Author(s)
Published by Oxford University Press on behalf of the Royal Astronomical Society

Downloaded from https://academic.oup.com/mnras/article/492/1/1/5603752 by guest on 12 December 2021

form of a spectacularly large and clumpy ring of about 200 kpc diameter around the ETG pair NGC 3384 and NGC 3379 (M105), and has no obvious ultraviolet (UV)/optical counterpart. It was thus long thought to have a primordial origin (Schneider et al. 1983, 1989; Schneider 1985). However, recent observations have found UV (Thilker et al. 2009), optical (Michel-Dansac et al. 2010), weak dust emission (Bot et al. 2009), and also metal-line absorption in the ring (Rosenberg et al. 2014). Stierwalt et al. (2009) in their Arecibo Legacy Fast ALFA (ALFALFA) observations of the Leo I group also identified about six candidate optical counterparts to the ring. However, only two of them, AGC 202027 and AGC 201970, had optical redshifts [from Sloan Digital Sky Survey (SDSS) and Karachentsev & Karachentseva (2004), respectively] close to the H I emission, and are thus associated with the ring. One of them, AGC 205505, has a slightly higher redshift than the H I emission from the ring, and is thus likely to be a background galaxy, although still a part of the M96 group (Stierwalt et al. 2009). The rest of the three galaxies AGC 201972 (also called KK94 in Karachentseva & Karachentsev 1998), AGC 202026, and AGC 201975 do not have redshift information to confirm the association with the ring. The metallicity of the Leo ring was found to be pre-enriched (Michel-Dansac et al. 2010; Rosenberg et al. 2014) suggesting a galactic origin. Recently, a very diffuse stellar object (BST 1047+1156) was found in the region connecting the Leo ring and M96 that could either be a tidal dwarf galaxy or a pre-existing extremely diffuse low surface brightness (LSB) galaxy (Mihos et al. 2018). Targeted simulations showed that the Leo ring could also have a collisional origin (Michel-Dansac et al. 2010). An alternative scenario for the formation of such massive, optically devoid H I clouds is the stripping of a gas-rich LSB galaxy with an extended H I disc by the tidal field of galaxy groups (Bekki et al. 2005).

Here, we report the discovery of a large (∼115 kpc in diameter) H I ring off-centred around a massive quenched galaxy, AGC 203001, using the Giant Metrewave Radio Telescope (GMRT). We also present deep optical *g*-, *r*-, and *i*-band imaging of the H I ring using the Canada–France–Hawaii Telescope (CFHT). In the context of this discovery, we discuss possible formation mechanisms for large H I rings.

Throughout this paper, we use the standard concordance cosmology from 9-year *Wilkinson Microwave Anisotropy Probe* (*WMAP*9; Hinshaw et al. 2013) with $\Omega_{\rm M} = 0.286$, $\Omega_{\Lambda} = 0.714$, and $h_{100} = 0.69$.

2 TARGET SELECTION

Our target, AGC 203001 (RA: $10^{\rm h}22^{\rm m}03\overset{\rm s}{.}315$, Dec.: $+13^{\circ}46'10\overset{''}{.}20$), belongs to a sample of quenched galaxies selected in the following manner. We first select galaxies with specific star formation rate [star formation rate (SFR)/stellar mass] below 10^{-11} yr^{-1} from the *Galaxy Evolution Explorer* (*GALEX*)–Sloan Digital Sky Survey (SDSS)–*Wide-field Infrared Survey Explorer* (*WISE*) Legacy Catalog (GSWLC; Salim et al. 2016). Such galaxies are designated as quenched galaxies (Salim 2014). Subsequently, we put a redshift cut of $z < 0.025$ on this sample to ensure sufficient spatial resolution with the GMRT and then we cross-match this sample with the optical counterparts identified from the single-dish ALFALFA (Haynes et al. 2018) H I survey. This resulted in a sample of 24 galaxies, of which 12 galaxies had early-type morphology and showed no signs of recent SF or interactions. From these, AGC 203001 was picked at random as a pilot object for observing the full sample with the GMRT. AGC 203001 is at a redshift of 0.01867 ($v_{\rm helio} = 5597$ km s^{-1}), has a stellar mass (M_*) of 1.5×10^{10} M$_{\odot}$ (Salim et al. 2016), and a S0 morphology (Nair & Abraham 2010). It has an SFR of 0.011 M$_{\odot}$ yr^{-1} that is very low for its stellar mass, and hence the galaxy is considered quenched. Yet, it has copious amounts of H I ($\log(M/{\rm M}_{\odot}) = 9.53 \pm 0.05$) as measured by the single-dish ALFALFA survey.

3 OBSERVATIONS AND DATA ANALYSIS

3.1 Deep H I imaging of AGC 203001

The GMRT 21-cm line observations of AGC 203001 were carried out on 2017 December 23 and 24 for a total on-source time of ∼10 h with the GMRT software backend. The total bandwidth was configured at 16.66 MHz divided into 512 channels, thus corresponding to a velocity resolution of ∼7 km s^{-1}, and centred at the heliocentric redshift of AGC 203001. The data analysis was carried out using standard tasks in the Astronomical Imaging Processing System (AIPS; Wells 1985) package. The initial flagging and calibration was done manually. Then a continuum image was made from the line-free channels that was used for self-calibration. After applying the self-calibration solution to the line visibilities, the continuum emission was subtracted using the task UVSUB. The cube was then imaged using the task IMAGR, and residual continuum was subtracted out using the task IMLIN. We reach a noise level of ∼0.67 mJy beam^{-1} for a velocity resolution of 14 km s^{-1} and with a beam size of 38.02×35.24 arcsec^2. The H I integrated intensity image and velocity field were made using the task MOMNT.

3.2 Deep optical imaging of the H I ring

On the publicly available images from optical imaging surveys such as DECam Legacy Survey (DECaLS) or Panoramic Survey Telescope and Rapid Response System (Pan-STARRS), the H I ring does not show any obvious optical counterpart. To check whether faint emission could nevertheless be associated, we have obtained deep multiband optical images of the field around AGC 203001 with the MegaCam camera installed on the CFHT. The observation and data reduction procedure that is optimized for the detection of low-surface brightness structures was the same as that used for the MATLAS/ATLAS$^{\rm 3D}$ survey (Duc et al. 2015). Final images were obtained with the ELIXIR-LSB software combining seven individual images acquired with relative offsets up to 20 arcmin, from which a master sky had been subtracted. Total exposure times were 34 min in the g' and r' bands, and 25 min in the i^* band. Weather conditions were photometric.

4 THE H I RING AROUND AGC 203001

We find that the H I in this galaxy is distributed in the form of a large ring around it, with a diameter of ∼115 kpc, as shown in blue contours in the left-hand panel of Fig. 1, with the optical *g*-, *r*-, and *i*-band colour composite image from CFHT in the background. Notice that the ring is asymmetrically distributed around the host galaxy. The right-hand panel in Fig. 1 shows the H I velocity map of the ring centred on AGC 203001, where we see that the ring shows some gradient in velocity. Table 1 describes some of the general properties of the H I ring.

There is no diffuse stellar emission along the H I ring in the CFHT MegaCam image going down to a depth of ∼28 mag arcsec^{-2}. In cases where there is *in situ* SF in the ring in the form of knots

Downloaded from https://academic.oup.com/mnras/article/492/1/1/5603752 by guest on 12 December 2021

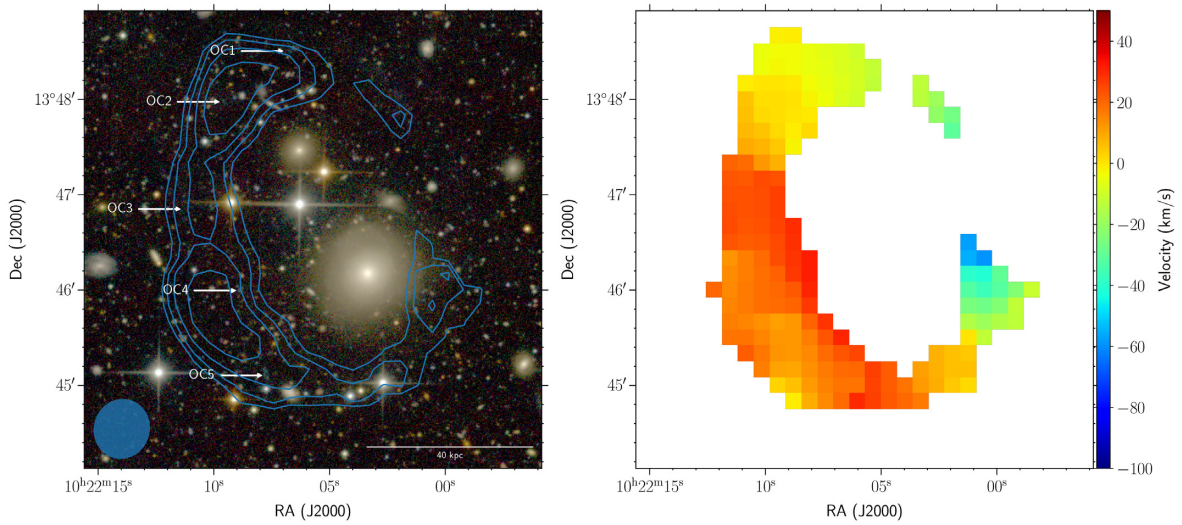

Figure 1. Left-hand panel: the H I ring around AGC 203001 in blue contours overlaid on the CFHT optical *g*-, *r*-, *i*-band colour composite image. The lowest contour corresponds to a H I column density of 2.8×10^{19} cm^{-2} and subsequent contours rise in multiples of $\sqrt{2}$. The H I ring has a projected diameter of ∼115 kpc. The arrows show the positions of the identified optical counterparts. Right-hand panel: the H I velocity map of the ring.

Table 1. General properties of the H I ring.

Total detected H I flux	1.13 ± 0.13 Jy km s^{-1}
Systematic velocity	5602.54 km s^{-1}
Velocity width	28.52 km s^{-1} (W50), 99.80 km s^{-1} (W20)
Ellipticity	0.67
Position angle of the major axis	20°
Peak column density	1.1×10^{20} cm^{-2}

we expect to find objects with relatively blue colours embedded particularly on the high column density regions of the ring. They are also expected to have a diffuse and irregular stellar distribution resembling dwarf irregular galaxies. Hence we visually inspected the region in and around the ring to search for the possible optical counterparts (OCs) to the ring. There are various objects coincident on the ring that mostly appear like background galaxies (which have evolved structures like bulges and discs). There are also several red barely resolved objects that are likely to be high-redshift galaxies. Interestingly, we also find several rather blue compact OCs close to several high column density H I condensations of the ring as denoted in Fig. 1. In Fig. 2, we show a zoom-in of the five OCs. We obtained their magnitudes using aperture photometry in IRAF. The magnitudes were then measured using circular apertures for all the OCs with a size of ∼3 times the full width at half-maximum (FWHM) using the PHOT task in the IRAF APPPHOT. The background was determined by making an annulus around the OCs. Table 2 summarizes the positions and magnitudes of all the OCs of the ring. Note that in the *i* band for all the OCs except for OC4 and in the *r* band for OC2 and OC3 we could not get a reliable measure of the magnitude due to poor signal-to-noise ratio. The $g - r$ colours for the OCs range from about 0.1 to 0.6 mag and are thus consistent with SF.

We estimated the integrated spectrum of the ring in our GMRT observations using the task BLSUM in AIPS. The total detected H I flux of the ring is 1.13 ± 0.13 Jy km s^{-1}, including the absolute 10 per cent calibrations errors. However, the total H I flux from the single-dish ALFALFA measurement around AGC 203001 is 2.14 ± 0.07 Jy km s^{-1}. We thus miss out a significant fraction (47 per cent) of the flux in our GMRT observations. In Fig. 3, we compare the integrated spectrum of the ring using our GMRT observations (solid line) with that of the single-dish ALFALFA measurements (dotted line). Notice that the missing flux is fairly uniformly distributed across velocity. Such a missing flux could be due to (1) calibration error, (2) excessive flagging of short baselines, or (3) a large fraction of the H I is distributed in an extended diffuse component that is resolved out. The point source fluxes in our GMRT continuum image are in good agreement with the NRAO VLA Sky Survey (NVSS; Condon et al. 1998) fluxes. Moreover, there was minimal flagging done in the short baselines. A similar flux recovery was observed in a GMRT follow-up of the ALFALFA observations of the gas-rich interacting galaxy groups NGC 3166/9 and NGC 871/NGC 876/NGC 877 by Lee-Waddell et al. (2012, 2014). Hence we believe that there is still a significant amount of diffuse H I surrounding AGC 203001 that is resolved out in our GMRT observations. A follow-up of this galaxy with a compact array [like the Karl G. Jansky Very Large Array (VLA) D-array] might help in detecting some of this flux.

Fig. 4 shows the larger field of view of the H I image of the ring and the galaxies around it. Here galaxies denoted by G2 (RA: 10$^{\rm h}$21$^{\rm m}$49$^{\rm s}$.584, Dec.: +13°42′45″.83; AGC 205059), G4 (RA: 10$^{\rm h}$22$^{\rm m}$21$^{\rm s}$.728, Dec.: +13°50′58″.67), and G1 (AGC 203001) are classified to be part of the same group based on the friends-of-friends group finding technique (Tempel et al. 2014). AGC 203001 along with G2 and G3 are also likely to be part of the loose group of three galaxies, WBL 263 (White et al. 1999) and USGC U292 with a virial radius of ∼0.72 Mpc (Ramella et al. 2002). H I is detected in G2, a known member of the group. Additionally, we also detect G3 (RA: 10$^{\rm h}$21$^{\rm m}$31$^{\rm s}$.94, Dec.: +13°41′22″.4) in H I. G3 is a dwarf galaxy that does not have spectroscopic data in the SDSS Data Release 15 (DR15; Aguado et al. 2019). From our H I detection we obtain a systemic velocity of ∼5525 km s^{-1}. Hence, G3 is at a similar distance as AGC 203001 and likely part of the group. Notice that along the north-west section of the ring we see a curved LSB feature in the *g*-band image that appears to be associated with the ring. However, it is slightly misaligned with the ring and is possibly Galactic cirrus emission.

Downloaded from https://academic.oup.com/mnras/article/492/1/1/5603752 by guest on 12 December 2021

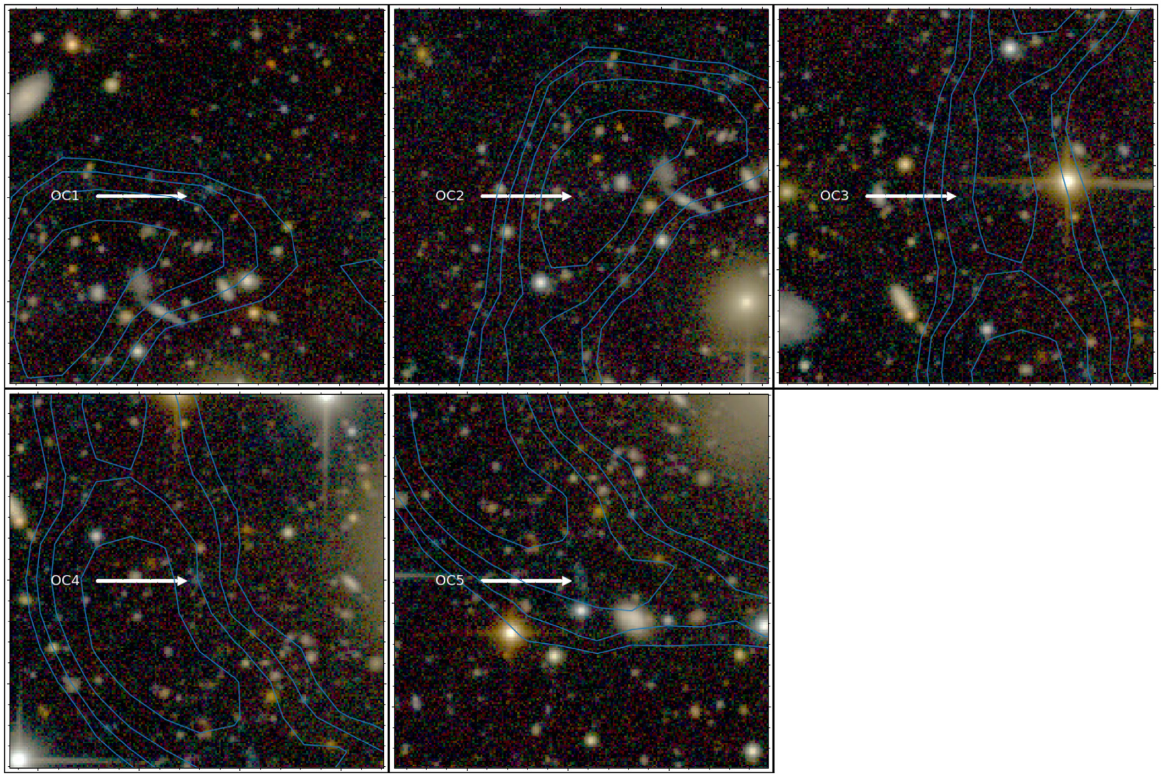

Figure 2. A 1.8 × 1.8 arcmin^2 zoom-in near the various optical counterparts of the ring. The H I column density contours are repeated from Fig. 1.

Table 2. Positions and magnitudes of optical counterparts to the ring.

ObjID	RA J2000 (°)	Dec. J2000 (°)	g (mag)	r (mag)	i (mag)
OC1	155.52844	13.80845	23.65 ± 0.18	23.04 ± 0.15	–
OC2	155.53990	13.79961	24.81 ± 0.40	–	–
OC3	155.54692	13.78085	25.65 ± 0.91	–	–
OC4	155.53694	13.76658	23.33 ± 0.12	23.26 ± 0.17	22.98 ± 0.28
OC5	155.53220	13.75176	23.51 ± 0.14	23.21 ± 0.13	–

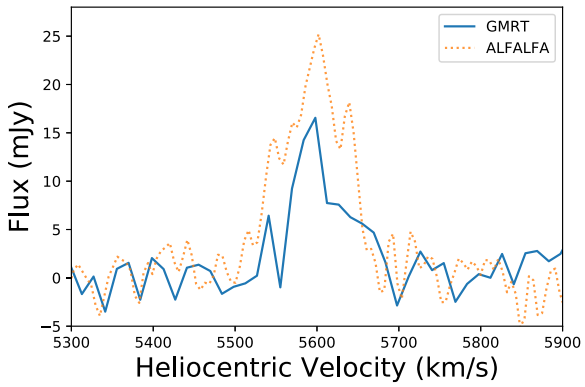

Figure 3. Comparison of the integrated spectrum of the ring from GMRT (solid line) with the ALFALFA spectrum (dotted line). The GMRT spectrum has about 47 per cent of the flux missing that is quite uniformly spread across the velocity. See text for details.

5 DISCUSSION

In this section, we show how the H I ring in this study compares with other known H I bearing ETGs, in particular the ATLAS^{3D} galaxies (Serra et al. 2012). We then briefly mention the possible formation scenarios for such a H I-dominated ring.

5.1 Comparison with H I observations of early-type galaxies

Here we use the H I gas fraction ($\log(M_{\rm H\,I}/M_*)$) versus near-UV (NUV) − r plane (Catinella et al. 2018) to see how AGC 203001 compares particularly with ATLAS^{3D} galaxies (which forms a representative sample for ETGs with H I) and other known H I bearing ETGs from the literature. The details of data selection are provided in Appendix A that is available as online supplementary material.

In Fig. 5, we compare AGC 203001 (red star) with ATLAS^{3D} galaxies shown in yellow points on the H I gas fraction versus NUV − r plane. For reference we show the median values from the

Downloaded from https://academic.oup.com/mnras/article/492/1/1/5603752 by guest on 12 December 2021

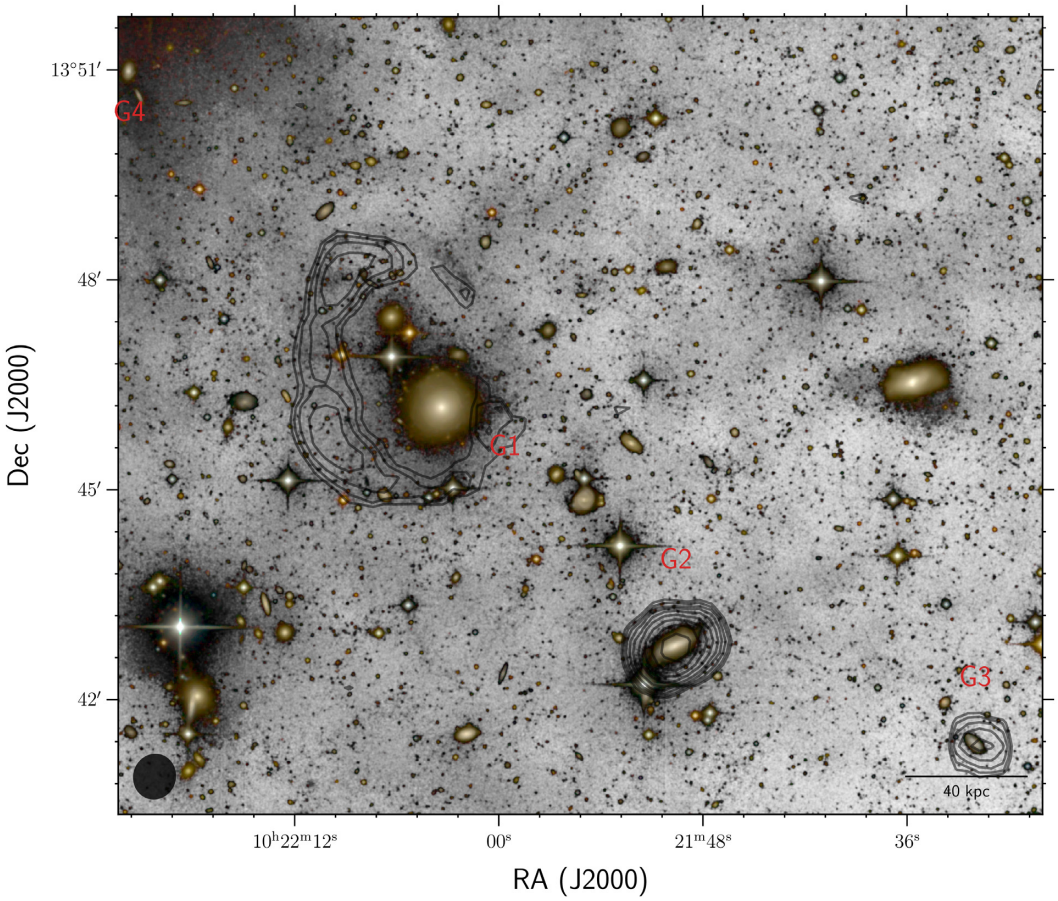

Figure 4. Large-scale image of the H I ring overlaid on the CFHT *g*-band image shown in reversed grey-scale wherein the background is shown in white and emission is shown in grey. The *gri* colour composite image is superimposed to identify the objects. The H I contours are shown in black with the contour levels repeated from Fig. 1. Here we show the two more sources for which we detected H I, denoted as G2 and G3. See text for more details.

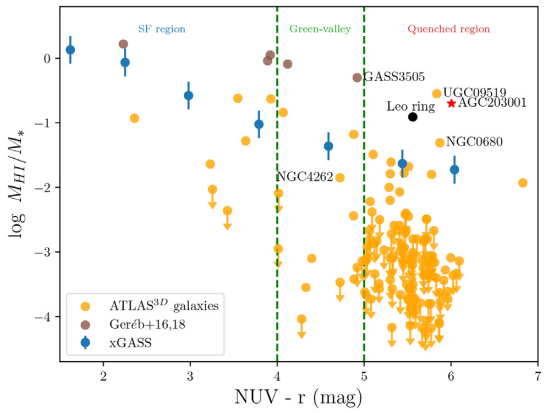

Figure 5. The H I gas fraction versus NUV − *r* plane. The blue points represent the median values from the xGASS survey (Catinella et al. 2018). AGC 203001 is marked with a red star and the Leo ring is marked with a black point. The yellow points represent the ATLAS^{3D} galaxies and the brown points represent the H I-excess galaxies (with GASS 3505 highlighted) from Geréb et al. (2016, 2018). The names of some of the H I-rich ATLAS^{3D} galaxies, UGC 09519 and NGC 0680, and a ring galaxy NGC 4262 are highlighted. The region within the green dashed line corresponds to the green-valley from Salim (2014), and the region on the left and right corresponds to the SF and quenched region, respectively. See text for discussion.

mass-selected extended *GALEX* Arecibo SDSS Survey (xGASS; Catinella et al. 2018). The green dashed lines differentiate the star-forming green-valley and quenched region (Salim 2014). Most of the ATLAS^{3D} galaxies are gas poor, particularly those in the quenched region. On the contrary, AGC 203001 is much more gas rich than ATLAS^{3D} galaxies and is in the quenched region (by virtue of its selection). And it is rather more close to the Leo ring, UGC 09519 and NGC 0680. We also show a sample of H I-excess galaxies with very low SF efficiency from Geréb et al. (2016, 2018) (shown in brown), with GASS 3505 highlighted. These galaxies were found to be outliers on the gas fraction versus NUV − *r* colour and stellar mass surface density. Compared to AGC 203001, these galaxies are much more gas rich and are relatively more star forming. We also highlight NGC 4262 (which is also part of the ATLAS^{3D} sample), a typical example of a barred lenticular galaxy with a H I ring (Krumm, van Driel & van Woerden 1985), which is classified as a polar ring galaxy by Khoperskov et al. (2014). In this case the H I ring shows a much more vigorous SF in the form of multiple star-forming knots (Bettoni, Buson & Galletta 2010).

One of the galaxies, NGC 0680 that is as H I rich as AGC 203001 is an interacting galaxy with an unsettled disc and thus has a very different morphology compared to AGC 203001 (Serra et al. 2012). The other galaxy, UGC 09519, is classified to have a large H I disc/ring morphology (Serra et al. 2012). However, H I disc/ring is well within the optical extent of the galaxy that is also very different

Downloaded from https://academic.oup.com/mnras/article/492/1/1/5603752 by guest on 12 December 2021

from AGC 203001. Moreover, in the relatively deeper Mayall *z*-band Legacy Survey/Beijing–Arizona Sky Survey (MzLS/BASS) images (Dey et al. 2019), it clearly shows a diffuse optical ring unlike in AGC 203001. The other case is that of the radio galaxy B2 0648+27. It has very large amount of H I mass ($\sim 1.1 \times 10^{10}$ $M_{\odot}$) distributed in the form of a large ring/disc extending ∼160 kpc and centred on the host galaxy (Morganti et al. 2003b), as against AGC 203001. Moreover, the host galaxy shows clear signs of a major merger in the deeper optical image due to a distorted optical morphology and tidal arms (Emonts et al. 2008). This again is different from the case of AGC 203001 presented here. We could not compare this galaxy in Fig. 5 due to lack of *GALEX* UV data. The Leo ring that is also an outlier in this gas scaling relation (close to AGC 203001) and also have a quenched host galaxy (even if we assume the host to be NGC 3379). More importantly, its H I morphology is in the form of a large off-centred ring extending ∼200 kpc (Schneider et al. 1983; Schneider 1985). It has no diffuse large-scale optical counterpart even in deep optical imaging (Michel-Dansac et al. 2010; Watkins et al. 2014). Only faint star-forming knots and diffuse structures were found within the ring in the UV (Thilker et al. 2007) and in the optical (Stierwalt et al. 2009; Michel-Dansac et al. 2010; Mihos et al. 2018) suggesting *in situ* SF. None of the galaxies in the Leo I group show any signs of recent interactions, except for NGC 3384 that might have undergone a minor merger (Watkins et al. 2014).

Thus the H I ring around AGC 203001 is unlike a typical ATLAS^{3D} galaxy, and has much more gas (due to its selection). In terms of its H I morphology it is rather closer to other known cases of giant H I rings around ETGs (e.g. the Leo ring and B2 0648+27). However, based on its optical properties it appears to most closely resemble the rare case of the Leo ring.

5.2 Possible formation scenarios for the ring around AGC 203001

The off-centre nucleus of the H I ring makes it a P-type ring based on the classification by Few & Madore (1986). These types of rings are thought to have a collisional origin with an intruder galaxy that is typically within two diameters of the ring. We identify a nearby galaxy (G2) at a projected distance of ∼109 kpc, which could be the possible intruder. A recent collision between G2 and the host galaxy at a relatively high speed could have triggered the formation of this ring. We also see asymmetrical outer isophotes in the optical image of the host galaxy that could be the signs of such an interaction. We note, however, that both the stellar and H I components of G2 do not show any signs of recent interaction.

In some aspects, our ring is strikingly different from typical collisional ring galaxies. It lacks any bright optical counterpart suggesting almost negligible amounts of past and current events of SF. The high SFRs in the more traditional rings are due to gas compression after the collision. In a recent simulation of Cartwheel-like ring galaxies it was shown that SF first takes place in the expanding ring, soon after the collision, due to the induced density wave (Renaud et al. 2018). However, the H I gas column density in our ring is much below the SF threshold (of $\sim 10^{21}$ cm^{-2}), thus suggesting that the gas may not have been sufficiently compressed after the collision to induce SF. Very locally, the gas density was high enough though to allow the onset of limited SF, indicated by the presence of the blue OCs.

We propose a possible explanation and alternative scenarios for our observations as follows. It is possible that the host galaxy was a H I-rich ETG, like those of the ATLAS^{3D} galaxies (Serra et al. 2012), which have low column density H I gas disc to begin with and hence low SF, which underwent a collision to form the ring. This can explain the low SFR in the host galaxy and the ring. Another natural solution for all the discrepancies is that the possible collision of the gas between the intruder and AGC 203001, may have imparted a strong shock that can heat the gas in the host to very high temperatures a possibility pointed out by Appleton & Struck-Marcell (1996). Such a heating of the gas may have prevented SF in the ring, leading to a more diffuse H I ring. The inclusion of such a shock heating in collisional ring galaxy simulations, an effect largely ignored until now, may provide extra parameter space to produce such a large and optically devoid H I ring.

Alternatively, as suggested by simulations in Bekki et al. (2005), such a ring-like structure could have formed due to tidal stripping of the outer gas from a LSB galaxy having an extended H I disc by the group potential. In their simulations, the H I gas column density is expected to be quite low and it lacks any SF that is consistent with our observations of the H I ring.

Major merger is yet another possibility for the formation of such a ring around AGC 203001. Morganti et al. (2003a,b) proposed an evolutionary sequence wherein large H I-rings/disc around ETGs could represent late stages of gas-rich mergers. In this scenario, the large-scale tidal tails around the Antennae galaxies (which is an ongoing merger) will eventually fall back in the centre forming a large diffuse disc/ring-like structure (like NGC 5266; Morganti et al. 1997). The host galaxy will undergo a starburst phase, followed by a possibly brief period of AGN activity (like B2 0648+27) and then eventually turn into a quenched ETG. In such a scenario, the ring around AGC 203001 would be placed in the late stage of the evolutionary sequence.

6 CONCLUSION AND FUTURE WORK

In conclusion, we have discovered an extremely rare example of a large off-centred H I ring, extending almost ∼115 kpc in diameter around AGC 203001. Our deep CFHT *g*-, *r*-, and *i*-band images show that this ring has several faint optical counterpart at surface brightness levels of ∼28 mag arcsec^{-2}. Conventionally, ring galaxies are thought to have a collisional origin, although they also predict large amounts of SF in it, which is contrary to our observations. The origin of such H I-dominated rings is still poorly understood. In the future, we hope to increase the number of such extended H I structures by mapping more galaxies found using our criteria that can help in understanding their formation scenario.

ACKNOWLEDGEMENTS

We thank the anonymous referee for several insightful comments that have improved both the content and presentation of this paper. OB would like to thank Nissim Kanekar for help with the GMRT data analysis. We thank the staffs of the GMRT who have made these observations possible. GMRT is run by the National Centre for Radio Astrophysics of the Tata Institute of Fundamental Research. Based on observations obtained with MegaPrime/MegaCam, a joint project of CFHT and CEA/DAPNIA, at the Canada–France–Hawaii Telescope (CFHT) that is operated by the National Research Council (NRC) of Canada, the Institut National des Sciences de l'Univers of the Centre National de la Recherche Scientifique of France, and the University of Hawaii. PK's work at RUB is partly supported by BMBF project 05A17PC2 for D-MeerKAT. This research has made use of APLPY, an open-source plotting package for PYTHON (Robitaille & Bressert 2012), MATPLOTLIB (Hunter 2007),

Downloaded from https://academic.oup.com/mnras/article/492/1/1/5603752 by guest on 12 December 2021

and ASTROPY,[1] a community-developed core PYTHON package for Astronomy (Astropy Collaboration et al. 2013; Price-Whelan et al. 2018). This research has also made use of NASA's Astrophysics Data System.

REFERENCES

Aguado D. S. et al., 2019, ApJS, 240, 23
Appleton P. N., Struck-Marcell C., 1987, ApJ, 318, 103
Appleton P. N., Struck-Marcell C., 1996, Fundamentals Cosmic Phys., 16, 111
Astropy Collaboration et al., 2013, A&A, 558, A33
Bekki K., Koribalski B. S., Ryder S. D., Couch W. J., 2005, MNRAS, 357, L21
Bettoni D., Buson L. M., Galletta G., 2010, A&A, 519, A72
Binney J., Tremaine S., 2008, Galactic Dynamics, 2nd edn. Princeton Univ. Press, Princeton, NJ
Bot C., Helou G., Latter W. B., Puget J., Schneider S., Terzian Y., 2009, AJ, 138, 452
Catinella B. et al., 2018, MNRAS, 476, 875
Condon J. J., Cotton W. D., Greisen E. W., Yin Q. F., Perley R. A., Taylor G. B., Broderick J. J., 1998, AJ, 115, 1693
de Vaucouleurs G., 1959, Handb. Phys., 53, 275
Dey A. et al., 2019, AJ, 157, 168
Duc P.-A. et al., 2015, MNRAS, 446, 120
Dyson F. W., 1893, Philos. Trans. R. Soc. Lond. Ser. A, 184, 43
Elagali A., Lagos C. D. P., Wong O. I., Staveley-Smith L., Trayford J. W., Schaller M., Yuan T., Abadi M. G., 2018, MNRAS, 481, 2951
Emonts B. H. C., Morganti R., van Gorkom J. H., Oosterloo T. A., Brogt E., Tadhunter C. N., 2008, A&A, 488, 519
Few J. M. A., Madore B. F., 1986, MNRAS, 222, 673
Geréb K., Catinella B., Cortese L., Bekki K., Moran S. M., Schiminovich D., 2016, MNRAS, 462, 382
Geréb K., Janowiecki S., Catinella B., Cortese L., Kilborn V., 2018, MNRAS, 476, 896
Haynes M. P. et al., 2018, ApJ, 861, 49
Hernquist L., Weil M. L., 1993, MNRAS, 261, 804
Hinshaw G. et al., 2013, ApJS, 208, 19
Hunter J. D., 2007, Comput. Sci. Eng., 9, 90
Karachentsev I. D., Karachentseva V. E., 2004, Astron. Rep., 48, 267
Karachentseva V. E., Karachentsev I. D., 1998, A&AS, 127, 409
Khoperskov S., Moiseev A., Khoperskov A., Saburova A. S., 2014, MNRAS, 441, 2650
Krumm N., van Driel W., van Woerden H., 1985, A&A, 144, 202
Lee-Waddell K., Spekkens K., Haynes M. P., Stierwalt S., Chengalur J., Chandra P., Giovanelli R., 2012, MNRAS, 427, 2314
Lee-Waddell K. et al., 2014, MNRAS, 443, 3601
Lynds R., Toomre A., 1976, ApJ, 209, 382
Mapelli M., Moore B., Ripamonti E., Mayer L., Colpi M., Giordano L., 2008, MNRAS, 383, 1223
Michel-Dansac L. et al., 2010, ApJ, 717, L143
Mihos J. C., Carr C. T., Watkins A. E., Oosterloo T., Harding P., 2018, ApJ, 863, L7
Morganti R., Sadler E. M., Oosterloo T., Pizzella A., Bertola F., 1997, AJ, 113, 937
Morganti R., Oosterloo T., Tadhunter C., Emonts B., 2003a, New Astron. Rev., 47, 273
Morganti R., Oosterloo T. A., Capetti A., de Ruiter H. R., Fanti R., Parma P., Tadhunter C. N., Wills K. A., 2003b, A&A, 399, 511
Morganti R. et al., 2006, MNRAS, 371, 157
Nair P. B., Abraham R. G., 2010, ApJS, 186, 427
Oosterloo T. A., Morganti R., Sadler E. M., Vergani D., Caldwell N., 2002, AJ, 123, 729
Oosterloo T. et al., 2010, MNRAS, 409, 500
Price-Whelan A. M. et al., 2018, AJ, 156, 123
Ramella M., Geller M. J., Pisani A., da Costa L. N., 2002, AJ, 123, 2976
Renaud F. et al., 2018, MNRAS, 473, 585
Robitaille T., Bressert E., 2012, Astrophysics Source Code Library, record ascl:1208.017
Rosenberg J. L., Haislmaier K., Giroux M. L., Keeney B. A., Schneider S. E., 2014, ApJ, 790, 64
Salim S., 2014, Serbian Astron. J., 189, 1
Salim S. et al., 2016, ApJS, 227, 2
Schneider S., 1985, ApJ, 288, L33
Schneider S. E., Helou G., Salpeter E. E., Terzian Y., 1983, ApJ, 273, L1
Schneider S. E. et al., 1989, AJ, 97, 666
Serra P. et al., 2012, MNRAS, 422, 1835
Snyder G. F. et al., 2015, MNRAS, 454, 1886
Stierwalt S., Haynes M. P., Giovanelli R., Kent B. R., Martin A. M., Saintonge A., Karachentsev I. D., Karachentseva V. E., 2009, AJ, 138, 338
Struck-Marcell C., Appleton P. N., 1987, ApJ, 323, 480
Tempel E. et al., 2014, A&A, 566, A1
Theys J. C., Spiegel E. A., 1977, ApJ, 212, 616
Thilker D. A. et al., 2007, ApJS, 173, 538
Thilker D. A. et al., 2009, Nature, 457, 990
van Driel W., van Woerden H., 1991, A&A, 243, 71
Watkins A. E., Mihos J. C., Harding P., Feldmeier J. J., 2014, ApJ, 791, 38
Wells D. C., 1985, in di Gesu V., Scarsi L., Crane P., Friedman J. H., Levialdi S., eds, Data Analysis in Astronomy. Plenum Press, New York, p. 195
White R. A., Bliton M., Bhavsar S. P., Bornmann P., Burns J. O., Ledlow M. J., Loken C., 1999, AJ, 118, 2014
Yıldız M. K., Serra P., Peletier R. F., Oosterloo T. A., Duc P.-A., 2017, MNRAS, 464, 329
Zwicky F., 1941, in Theodore von Kármán Anniversary Volume: Contributions to Applied Mechanics and Related Subjects. California Institute of Technology, Pasadena, p. 137

SUPPORTING INFORMATION

Supplementary data are available at *MNRAS* online.

Appendix A. Details of the Data Selection for the Comparison with other H I Bearing ETGs.

Please note: Oxford University Press is not responsible for the content or functionality of any supporting materials supplied by the authors. Any queries (other than missing material) should be directed to the corresponding author for the article.

This paper has been typeset from a TEX/LATEX file prepared by the author.

[1] http://www.astropy.org

Downloaded from https://academic.oup.com/mnras/article/492/1/1/5603752 by guest on 12 December 2021